Metal-support Interactions and C1 Chemistry: Transforming Pt-CeO_2 into a Highly Active and Stable Catalyst for the Conversion of Carbon Dioxide and Methane

Feng Zhang,[a] Ramón A. Gutiérrez,[b] Pablo G. Lustemberg,[c,d] Zongyuan Liu,[e] Ning Rui,[e] Tianpin Wu,[f] Pedro J. Ramírez,[b,g] Wenqian Xu,[f] Hicham Idriss,[h] M. Verónica Ganduglia-Pirovano,*[d] Sanjaya D. Senanayake,*[e] and José A. Rodriguez*[a,e]

[a] Department of Materials Science and Chemical Engineering, SUNY at Stony Brook, Stony Brook, NY 11794 (United States)
[b] Facultad de Ciencias, Universidad Central de Venezuela, Caracas 1020-A (Venezuela)
[c] Instituto de Fisica Rosario (IFIR), CONICET-UNR, Bv. 27 de Febrero 210bis, S2000EZP Rosario, Santa Fe, (Argentina)
[d] Instituto de Catálisis y Petroleoquímica, CSIC, C/Marie Curie 2, 28049 Madrid (Spain)
[e] Chemistry Division, Brookhaven National Laboratory, Upton, NY 11973 (United States)
[f] X-ray Science Division, Advanced Photon Source, Argonne National Laboratory, Argonne, Illinois 60439 (United States)
[g] Zoneca-CENEX, R&D Laboratories, Alta Vista, 64770 Monterrey (México)
[h] SABIC Corporate Research & Development (CRD), KAUST, Thuwal, 29355 (Saudi Arabia)

*Corresponding authors: M. Verónica Ganduglia-Pirovano (vgp@icp.csic.es); Sanjaya D. Senanayake (ssenanay@bnl.gov); José A. Rodriguez (rodrigez@bnl.gov)

ABSTRACT

There is an ongoing search for materials which can accomplish the activation of two dangerous greenhouse gases like carbon dioxide and methane. In the area of C1 chemistry, the reaction between CO_2 and CH_4 to produce syngas (CO/H_2), known as methane dry reforming (MDR), is attracting a lot of interest due to its green nature. On Pt(111), elevated temperatures are necessary to activate the reactants and massive deposition of carbon makes this metal surface ineffective for the MDR process. In this study, we show that strong metal-support interactions present in Pt/CeO_2(111) and Pt/CeO_2 powders lead to systems which can bind well CO_2 and CH_4 at room temperature and are excellent and stable catalysts for the MDR process at moderate temperature (500 ºC). The behaviour of these systems was studied using a combination of *in-situ*/*operando* methods (AP-XPS, XRD, XAFS) which pointed to an active Pt-CeO_{2-x} interface. In this interface, the oxide is far from being a passive spectator. It modifies the chemical properties of Pt, facilitating improved methane dissociation, and is directly involved in the adsorption and dissociation of CO_2 making the MDR catalytic cycle possible. A comparison of the benefits gained by the use of an effective metal-oxide interface and those obtained by plain bimetallic bonding indicates that the former is much more important when optimizing the C1 chemistry associated with CO_2 and CH_4 conversion. The presence of elements with a different chemical nature at the metal-oxide interface opens the possibility for truly cooperative interactions in the activation of C-O and C-H bonds.

Key words: C1 chemistry; CO_2 conversion; CH_4 conversion; methane dry reforming; platinum; metal-support interactions

TOC

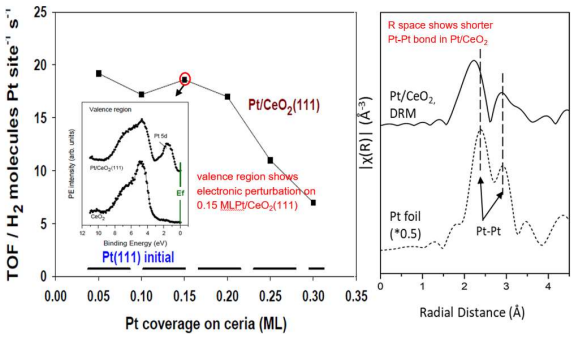
TOF / H2 molecules Pt site-1 s-1
Pt coverage on ceria (ML)
Pt/CeO2(111)
valence region shows
electronic perturbation on
0.15 MLPt/CeO2(111)
Pt(111) initial
Valence region
Pt 5d
Ef
Binding Energy (eV)
R space shows shorter
Pt-Pt bond in Pt/CeO2
Pt/CeO2,
DRM
Pt foil
(*0.5)
Pt-Pt
|χ(R)| (Å-3)
Radial Distance (Å)

Introduction

Carbon dioxide (CO_2) is a common greenhouse gas emitted whenever coal, oil or other carbon-rich fuels are burned. It is the largest contributor to climate change.[1] The conversion of CO_2 to high value chemicals or fuels is an important topic which is attracting a lot of attention worldwide. Methane (CH_4) is the simplest, most stable and abundant alkane molecule in our planet. While methane does not linger as long in the atmosphere as carbon dioxide, it is far more devastating to the climate because of how effectively it absorbs heat.[3-5] CH_4 has a green-house warming potential (GWP) which is 84 times greater than that of CO_2. It has been estimated that methane can be responsible for 25% of already observed changes to Earth's climate.[3-5] CH_4 is the main component of natural gas and is frequently flared or vented into the atmosphere in oil and gas drilling operations. As in the case of CO_2, there is a broad interest in the activation and conversion of methane into value added chemicals (aromatics, olefins, oxygenates).[2,4-5]

In the area of C1 chemistry, the reaction between CO_2 and CH_4 to produce syngas (CO/H_2), methane dry reforming (MDR), has attracted a lot of interest due to its green nature.[6] The syngas produced by this reaction can be used in fuel cells fed with H_2, in the synthesis of methanol or other oxygenates, and in the production of hydrocarbons through the Fischer-Tropsch process.[6] Two main reactions in the MDR process involve the conversion of CO_2:

$$CO_2 + CH_4 \rightarrow 2CO + 2H_2 \quad (\Delta H_{298K} = 247\ kJmol^{-1}) \quad (1)$$

$$CO_2 + H_2 \rightarrow CO + H_2O \quad (\Delta H_{298K} = 41\ kJmol^{-1}) \quad (2)$$

The second reaction, the reverse water-gas shift (RWGS), is often seen at high temperature. The MDR process is a real challenge due to the high stability and the non-polar nature of both CO_2 and CH_4.[2,7-9] Heterogeneous catalysts are frequently used to accomplish this task and the activation of C-O and C-H bonds must be done in a concerted

manner to avoid carbon deposition and subsequent deactivation of the catalyst.[6, 8] When dealing with the activation of CO_2 and CH_4 on metal and oxide surfaces, several descriptors and scaling relations have been examined for the controlled cleavage of the C-O or C–H bonds in these molecules.[7-15] But, what types of systems can activate simultaneously CO_2 and CH_4? It has become clear that single metals alone are not efficient for the MDR process[16-17] and better results can be obtained when one uses metal-metal or metal-oxide interfaces where different sites cooperate in the activation of CO_2 and CH_4.[8, 18-20]

In recent years, great research efforts are being done in order to develop metal/oxide catalysts with good activity, selectivity and stability for the MDR process.[6, 8] Systems which contain noble metals (Rh, Ru, Pt and Ir) have received substantial attention since they can be very active and less sensitive to deactivation by carbon deposition than catalysts based on Ni or Co.[6, 21-24] Pt and Pt-alloys have been investigated showing a remarkable potential,[6, 25-29] but important issues such as the effect of the metal particle size or morphology and the role of the oxide support (Al_2O_3, MgO, CeO_2, ZrO_2, CeO_2-ZrO_2, carbon) need to be addressed for optimizing this type of MDR catalysts.[6] In this article, we investigate the MDR process on well-defined Pt/CeO_2(111) and powder Pt/CeO_2 catalysts using a multi-technique approach.

On surfaces of noble metals, methane exhibits a rather low probability for dissociation which makes difficult the effective conversion of the molecule.[30-32] For example, on clean Pt(111), a typical benchmark surface for hydrocarbon activation, the methane C–H dissociation probability is close to 1×10^{-8} at 25 °C.[32] At this temperature, the hydrocarbon molecule dissociates depositing C and CH_3 species on the platinum surface. Upon heating to 100-200 °C, the formation of C–C bonds occurs generating species such as ethylidyne (C_2H_3) and ethynyl (C_2H) on the platinum surface.[32] A

carbonaceous layer eventually deactivates the chemical and catalytic properties of Pt(111).[32] The same occurs when Pt(100) or Pt(110)-(1x2) are exposed to methane at elevated temperature.[33-34] The platinum surfaces are also very poor for the activation of CO_2.[7] Neither Pt(111) nor Pt(100) bind well carbon dioxide.[7] Recent studies point to special electronic and chemical properties for Pt atoms in contact with ceria,[35-37] but no systematic study has been performed for the reaction of CO_2 and CH_4 over Pt-CeO_2 interfaces. Can metal-support interactions be useful for MDR and in the control of carbon deposition on platinum? In this article, we show clear evidence of metal-support interactions in the Pt/CeO_2 system and their effects in shifting the system away from the normal behaviour of bulk Pt, producing active and stable catalysts for CO_2 and CH_4 activation in dry reforming.

Results and Discussion

Reaction of CH_4 and CO_2 on Pt/CeO_2(111) surfaces. We started by investigating the interaction of CH_4, CO_2 and CH_4/CO_2 mixtures with Pt/CeO_2(111) surfaces. Figure 1 shows valence photoemission spectra for a clean CeO_2(111) surface and a surface containing 0.15 monolayer (ML) of platinum. The valence spectrum for the ceria system exhibits the O 2p band between 8 and 3.5 eV with a large band gap below the Fermi level (E_f). The addition of the Pt led to the appearance of new features centred at a binding energy of 2 to 1 eV. These features come from Pt 5d, 6s states. It is important to notice that the density of states (DOS) around the Fermi level for Pt/CeO_2(111) is close to zero. This is very different from the valence photoemission spectrum of bulk platinum, Pt(111) or Pt(100), where a very large DOS is seen at the Fermi level.[37,38-39] Thus, the Pt atoms in contact with ceria exhibit very strong electronic perturbations which can affect their chemical and catalytic properties. This phenomenon was seen over a wide range of

temperatures (25-600 °C) but only at small coverages of Pt (< 0.2 ML). For higher coverages of the admetal (> 0.5 ML), the valence spectrum of Pt/CeO_2(111) eventually converged to that of bulk platinum and the novel chemical behaviour of the admetal disappeared.[37] The UPS data at low Pt coverages are consistent with previous theoretical studies which show electronic perturbations when atoms or small clusters of the metal are in contact with a ceria surface.[33-35,40,41]

The top panel in Figure 2 shows C 1s XPS spectra collected after exposing plain CeO_2(111) and surfaces pre-covered with 0.15 and 0.25 ML of platinum to 1 Torr of CH_4 at 25 °C. CeO_2(111) did not dissociate the hydrocarbon molecule at 25 °C. However, methane dissociation occurred in the case of Pt/CeO_2(111). A peak around 284.8 eV points to the presence of CH_x (x= 1,2,3) fragments on the surface produced by the partial dissociation of methane ($CH_4 \rightarrow CH_x + (4\text{-}x)\ H$).[18-20] A second peak around 290 eV indicates the formation of carbonate-like CO_x species as a consequence of the full dissociation of methane.[18-20] The Pt/CeO_2(111) surfaces in Figure 2 exhibit a reactivity towards methane higher than that seen for surfaces of the bulk metal such as Pt(111), Pt(100) or Pt(110)-(1x2).[31-34]

The reactivity of the Pt/CeO_2(111) surfaces to dissociate methane at 25 ºC depended strongly on the amount of platinum dispersed on ceria. The highest reactivity was seen for the system with 0.15 ML (see Figure 2). This correlates with the large electronic perturbations seen in valence photoemission (Figure 1). At higher coverages of Pt (> 0.2 ML), the electronic perturbations on Pt decreased,[37] and the amount of CH_x and CO_x deposited on the surface upon exposure also dropped (bottom panel in Figure 2). Previous theoretical studies have indicated that electronic perturbations associated with Pt-CeO_2 bonding can largely reduce the barrier for the activation of C-H bonds in methane.[42]

Figure 3 displays C 1s XPS spectra collected after exposing plain $CeO_2(111)$ and a ceria surface pre-covered with 0.15 ML of platinum to 1 Torr of CO_2 at 25 °C. For both systems, the adsorption of CO_2 produces a peak around 290 eV which can be assigned to a carbonate (CO_x) species produced by direct reaction of CO_2 with O sites of the surface.[18-20] The presence of Pt did not lead to the growth of clear peaks for adsorbed CO_2 or CO on the metal, but the occurrence of a reaction of the CO_2(gas) → CO(gas) + O(surface) type cannot be ruled out. XPS showed that the platinum was oxidized from mainly Pt^{1+} to Pt^{2+} upon exposure to CO_2. This is remarkable because neither Pt(111) nor Pt(100) bind carbon dioxide well.[7] The similarities of the carbonate peaks in Figure 3 suggests that the adsorbed CO_2 mainly interacted with the ceria support. Thus, our XPS results indicated that CH_4 and CO_2 can be adsorbed on $Pt/CeO_2(111)$ at room temperature, but they did not react to yield syngas as expected by the MDR process. Catalytic activity was observed at temperatures above 400 °C after the methane reduced the ceria producing O vacancies where CO_2 dissociated.

A batch reactor was used to test the catalytic performance of plain Pt(111), $CeO_2(111)$, and 0.15 ML of Pt deposited on a $CeO_2(111)$ surface. At the reaction conditions examined (1 Torr of CH_4, 1 Torr of CO_2, 400-500 °C), neither Pt(111) nor $CeO_2(111)$ showed any sustained activity for the MDR reaction. In the case of Pt(111), some catalytic activity was initially observed but it dropped continuously and, after 20 minutes of reaction, no catalytic activity was seen (Figure 4). Post-reaction characterization with XPS showed that the plain platinum surface was poisoned by a thick carbon layer generated by the decomposition of methane. On this system, the CO_2 could not dissociate fast enough to provide the O for the removal of the carbon generated by methane.[32] In addition, Pt(111) is known to be active for the Boudouard reaction ($2CO \rightarrow C + CO_2$) which also could induce platinum deactivation by carbon poisoning.

In contrast to the behaviour of Pt(111), our kinetic data shown in Figure 4 indicate that a catalyst generated by depositing 0.15 ML of Pt on a CeO_2(111) surface is highly active and stable for the MDR reaction. The metal-support interactions in the Pt-CeO_2 interface lead to an excellent catalytic performance. Furthermore, these interactions also substantially reduce the rate of the Boudouard reaction with respect to Pt(111).[37] Thus, both factors make Pt/CeO_2(111) a very good catalyst for the MDR process. Post-reaction characterization with XPS gave a negligible amount of C on Pt/CeO_2(111) after 30 minutes of reaction under MDR conditions. In the C1s XPS region, a peak for carbonate, similar to that seen in Figure 3, was seen. Furthermore, upon finishing the post-reaction characterization with XPS, the sample was transferred back to the reactor and the MDR process was performed under the same conditions of Figure 4 for an additional two hours, observing the same rate of H_2 production and no measurable deposition of carbon on the surface of the catalyst.

Figure 5 displays the calculated turnover frequency (TOF) at 500 °C for different Pt/CeO_2(111) systems as a function of admetal coverage. The TOFs were calculated assuming that all the Pt atoms which were present on the ceria support were active in the catalytic process. For comparison, in Figure 5, we also include the initial TOF for Pt(111) before its surface was deactivated by carbon deposition. Results of Figure 5 indicate that at small coverages of Pt, the dispersed particles on ceria are at least 20 times more active than plain Pt(111). Thus, the remarkable increase in the activity and stability of Pt might be linked to the strong interactions of small coverages of Pt with CeO_2. In Figure 5, the TOF decreases when the Pt coverage goes above 0.2 ML. A phenomenon which correlates with a reduction in the electronic perturbations[37] in Pt and in the reactivity of the admetal towards methane (Figure 2).

AP-XPS was used to study the chemical state of a $Pt/CeO_2(111)$ catalyst when exposed to a reactant CH_4/CO_2 mixture in a large range of temperatures (Figure 6). The initial position of the Pt 4f peak indicates that Pt is oxidized with a Pt^+ dominating feature upon deposition on $CeO_2(111)$ at 25 °C.[40-42] The exposure to the CH_4 and CO_2 gas mixture induced a peak shift of the Pt signal to higher binding energy at 25 and 127 °C. This peak shift could be attributed to the adsorbed CO_x/CH_x species (resulting from CH_4 dissociation and CO_2 binding, see Figures 2 and 3) on the Pt surface which increased the work function and binding energy.[43-44] An analysis of the corresponding Ce 3d XPS spectra indicates that there may be some reduction of Ce^{4+} into Ce^{3+} upon exposure to the CH_4/CO_2 gas mixtures at different temperatures. As can be seen, upon the deposition of Pt, most of the ceria is in the 4+ state, and the decline of the Ce^{4+} $3d_{3/2}$ signal (peak at ~909 eV) at 25 and 127 °C under the MDR reaction condition indicates a slight reduction of Ce^{4+}. This phenomenon was not observed on other similar 0.15 ML $M/CeO_2(111)$ (M=Co, Ni, Cu) catalysts,[19] implying a much stronger metal-support interactions in the $Pt/CeO_2(111)$ system. In addition, the slight reduction observed on the ceria support at 25 °C also manifests the increased reducibility of ceria when Pt was loaded, as there is no sign for CH_4 dissociation on pure CeO_2 at 25 °C as shown in Figure 2. This increased reducibility was also verified on the Pt/CeO_2 powder system, as can be seen in Figure S1, the loading of Pt on the ceria support significantly decreased the temperature needed to reduce the surface of ceria.

In Figure 6, as the temperature increases, a total shift of the Pt signal to lower binding energy at 327 and 427 °C was observed in the AP-XPS spectra, indicating the reduction of $Pt^{\delta+}$. And under the active MDR reaction conditions (> 400 °C), metallic Pt is present in the surface of the catalyst.[40-41] The Ce^{4+} peak (at ~909 eV) also grows at 227 °C and the signal of Ce^{3+} is negligible until 427 °C under the MDR reaction condition.[45]

In test experiments, we found that plain methane reduces ceria in the $Pt/CeO_2(111)$ system at elevated temperatures (~23% of Ce^{4+} was reduced to Ce^{3+} at 427 °C, see Figure S2 and Table S1), but the formed Ce^{3+} re-oxidized fast back to Ce^{4+} upon exposure to CO_2. This indicates that a balanced redox cycle was achieved on the ceria support when the sample was exposed to the MDR reaction atmosphere. In general, under the active MDR reaction conditions, an interface containing small particles of Pt dispersed on a reactive ceria support is the active phase of the MDR catalyst.

Reaction of CH_4 and CO_2 on a Pt/CeO_2 powder. Previous studies of AP-XPS and time-resolved X-ray diffraction have shown that a Pt/CeO_2 powder is also effective for the low temperature activation of methane.[42] Thus, we decided to test such a system in the conversion of CO_2/CH_4, and investigate the possible metal-support interactions in the Pt/CeO_2 powder system under MDR reaction conditions. Tests in a flow reactor showed that a 0.5 wt% Pt/CeO_2 powder was active and stable as an MDR catalyst at 500 °C with a very good performance at even higher temperatures (Figure 7). In the tests of Figure 7, CO_2 was consumed by the MDR and the reverse water-gas shift ($CO_2 + H_2 \rightarrow CO + H_2O$) reactions. At 500 °C, the conversion of CH_4 and CO_2 was 7 and 13%, respectively, with the system remaining stable for more than 20 hours. The production rate of H_2 and CO was 27 and 84 $\mu mol/g_{cat}/s$, respectively at 500 °C, and reached to 475 and 650 $\mu mol/g_{cat}/s$ at 700 °C.

A combination of *in-situ* measurements with AP-XPS, XAFS and XRD was used to fully characterize the 0.5 wt% Pt/CeO_2 powder catalyst under reaction. The AP-XPS results are summarized in Figure 8. Any $Pt^{\delta+}$ feature present on the samples at 25 °C was pre-reduced in H_2 so that active metallic Pt was present on the catalysts surface for the MDR process. The pre-reduced Pt^0 maintains its metallic feature throughout the MDR reaction at elevated temperatures. In the Ce 3d XPS region, the pre-treatment process

induced a partial reduction of Ce^{4+} to Ce^{3+}, however, after switching gas to the MDR reaction gas mixture at 25 °C, part of the Ce^{3+} re-oxidized back to Ce^{4+} by CO_2, and under the reaction conditions, the Ce^{4+} and Ce^{3+} kept a relatively stable ratio at elevated temperatures. On the surface of this catalyst, one probably had a dynamic redox process under the MDR reaction conditions, where methane or the H produced by methane dissociation reduced some Ce^{4+} to Ce^{3+}, which was then partially re-oxidized back by the dissociation of CO_2.

A reduction of the supported platinum was also observed in XANES and EXAFS measurements collected for the powder Pt/CeO_2 catalyst using a flow reactor and the regular conditions for the MDR process. The Pt L_3 edge XANES and the Fourier transformed EXAFS spectra are presented in Figure 9. PtO_2 (Pt^{4+}) was identified as a dominant structure in the as-prepared Pt/CeO_2 powder sample,[46-48] see Figure 9a. The strong Pt-O feature in the EXAFS spectrum of the pristine sample which aligns with the Pt-O characteristic peak of the PtO_2 reference also confirms the initial presence of PtO_2 in the bulk.[49] After H_2 reduction, PtO_2 was converted to metallic Pt, which remained until 700 °C under the MDR reaction. In Figure 9b, a peak shift of ~ 0.19 Å in the Pt-Pt shell was observed for the H_2 pre-treated sample and the sample under MDR condition. This leftwards shift implies shorter Pt-Pt bond distance of the small Pt clusters when they are supported on ceria, which evidenced the modification of Pt by the ceria support through the metal-support interactions in the powder Pt/CeO_2 system.

Figure 10 shows *in-situ* XRD data for 0.5 wt% Pt/CeO_2 under the MDR process. Only diffraction features for ceria are observed in Figure 10a because the Pt particles are too small (< 2 nm) to yield diffraction lines. Rietveld refinement allowed us to track variations in the ceria lattice (Figure 10b). The XRD measurements point to an expansion of the ceria lattice indicating a reduction of the ceria support, which is also consistent

with the existence of some Ce^{3+} in the powder catalyst as seen in AP-XPS (Figure 8). The ceria support was partially reduced by H_2 with a 0.02 Å lattice expansion (from 5.41 to 5.43 Å) during the H_2 pre-treatment process. After switching the feed from H_2 to an MDR reaction gas mixture at 25 °C, the ceria lattice decreased to 5.42 Å, indicating the partial re-oxidation of the ceria support by CO_2 at room temperature. Under the MDR reaction conditions, the ceria lattice expanded at elevated temperatures, following the thermal expansion trend of ceria, and after cooling down the sample back to 25 °C, the ceria lattice contracted back to the same value as before the MDR reaction. When compared to the total lattice expansion of ceria under a pure CH_4 gas environment from 25 to 700 °C (0.11 Å, in additional test measurements, shown in Figure S3), this result suggests that the partial reduction of the ceria support preserved a stable Ce^{3+} to Ce^{4+} ratio under the MDR reaction conditions (consistent with the results shown in Figure 8), and this implied that a balanced redox process, induced by simultaneous CH_4 and CO_2 decomposition, was achieved on the ceria support. This balanced redox process, also observed on the $PtCeO_2(111)$ model catalyst, is essential for the catalytic reaction. Although both reactants adsorb on the catalysts surface at 25 °C (Figures 2 and 3), a stable catalytic cycle is only established at elevated temperatures when methane or H produced by the dissociation of methane is able to reduce the ceria forming Ce^{3+} sites which are effective for the dissociation of CO_2.

Comparison to other metal/oxide catalysts for the MDR process. Small particles of Pt in contact with ceria display special electronic properties (UPS data, Figure 1) and shorter Pt-Pt distances (EXAFS data, Figure 9) with respect to bulk Pt. These results are consistent with findings of previous studies examining the interaction of Pt atoms or small metal clusters with ceria.[35-37,45] The electronic and structural perturbations affect the reactivity of the supported Pt particles. The results discussed above illustrate the

cooperative interactions which can occur when a metal-oxide interface is used for the activation of CH_4 and CO_2 in a dry reforming process.

In general, surfaces of pure platinum are not efficient for the activation of methane or carbon dioxide.[7,32-34] The metal component alone cannot carry out the chemistry and the oxide modifies the catalytic properties of the metal and participates in key reaction steps. In principle, the catalytic properties of the metal-oxide interface can be altered by changing its metal or oxide components. Figure 11 compares the catalytic activity of $Pt/CeO_2(111)$ and a series of $M/CeO_2(111)$ surfaces (M= Cu, Ni or Co) at an admetal coverage of ~ 0.15 ML.[18-20] The high activity of Ni/CeO_2 is remarkable,[50-52] however, the surfaces with Co and Pt are clearly the best catalysts, with Pt being more selective than Co since it does not form ethane or ethylene during the MDR process, as it is the case with Co.[19] Thus, in Pt/CeO_2 one has the best metal-ceria system with high activity, stability and selectivity.

In general, when optimizing the performance Pt MDR catalysts scientist has followed two different approaches: changing the oxide support (Al_2O_3, MgO, CeO_2, ZrO_2, CeO_2-ZrO_2) and alloying Pt with a second metal (Fe, Co, Ni, Cu). [6, 25-29,53-55] Our results show the important role that ceria plays as an active support/participant in the MDR process. It is superior with respect to Al_2O_3 and MgO because these oxides usually do not interact strongly with supported metals like ceria does. Pure ZrO_2 does interact with metals and produces an active ZrO_2/Pt interface for the MDR reaction,[53] but it does not have the redox properties of ceria which facilitate the dissociation of CO_2 and its incorporation within a catalytic cycle. On the other hand, zirconia-doped ceria is an interesting support because it interacts well with metals and its redox properties (Ce^{4+} to Ce^{3+} switching) could be enhanced with respect to plain ceria; the increased stability

against filamentous coke formation has also been reported on a Ni based catalyst. [6, 25, 27, 54-55]

Typically, surfaces of pure platinum {Pt(111), Pt(100), or Pt(110)-(1x2)} interact poorly with methane and, at the high-temperatures in which the breaking of C-H bonds is efficient, they become rapidly covered by a carbonaceous layer which leads to chemical and catalytic deactivation.[31-34] The formation of metal-metal interfaces, or alloys, is an approach which is frequently used to prevent coke generation and subsequent deactivation during the MDR process.[6,8] Pt is usually alloyed with a second metal (Ni, Co, Rh, Ru or Ir) to increase the activity of the system for CO_2 dissociation or to prevent carbon deposition and catalyst deactivation. [6, 25-26, 28-29] In our Pt/CeO_2 system, only a very small amount of Pt (0.15 ML and 0.5 wt%) was needed, and the chemical performance of the metal was promoted by interactions with the active oxide support, with the ceria also helping in the dissociation of CO_2. The results in Figures 2 and 3 are really remarkable because the common alloys of Pt investigated so-far were not able to bind well or activate in an effective way CO_2 and CH_4 at room temperature.[6, 25-29, 56-57] The TOFs seen in Figure 5 (17-19 H_2 molecules produced site^{-1} s^{-1}) are much larger than typical TOFs obtained after alloying Pt with a second metal (2-5 H_2 molecules produced site^{-1} s^{-1}).[29, 58-59] Thus, optimizing metal-support interactions and using an active oxide support seem as a much more efficient approach than plain bimetallic bonding when one wants to produce a highly active, selective and stable catalysts for the MDR process.

CONCLUSIONS

Pt(111) reacts poorly with carbon dioxide and methane. Elevated temperatures are necessary to activate these molecules and a massive deposition of carbon made this pure metal surface useless for the MDR process. The deposition of small Pt particles on ceria produces systems with short Pt-Pt distances and induces large electronic perturbations in

the valence states of the admetal, evidencing strong metal-support interactions in $Pt/CeO_2(111)$ and Pt/CeO_2 powders, leading to systems which bind well CO_2 and CH_4 at room temperature and are excellent and stable catalysts for the MDR process at moderate temperatures (500 ºC). Studies with *in-situ* or *operando* methods (AP-XPS, XRD, XAFS) point to an active $Pt\text{-}CeO_{2-x}$ interface. In this interface, the oxide is not only a passive spectator. It modifies the chemical properties of Pt, facilitating methane dissociation, and is directly involved in the adsorbing and dissociation of CO_2, making the MDR catalytic cycle possible. A comparison of the benefits gained by the use of an effective metal-oxide interface and those obtained by plain bimetallic bonding indicates that the former is much more important when optimizing the C1 chemistry associated with CH_4 and CO_2 conversion. The presence of elements with a different chemical nature at the metal-oxide interface opens the possibility for truly cooperative interactions in the activation of C-H and C-O bonds.

METHODS

Studies with well-defined $Pt/CeO_2(111)$ surfaces

The experiments examining the activation of CH_4 and its conversion by reaction with CO_2 on $Pt/CeO_2(111)$ surfaces were performed in a set-up that combined an ultra-high vacuum (UHV) chamber for surface characterization and a micro-reactor for catalytic tests.[18-19, 37] The UHV chamber was equipped with instrumentation for X-ray photoelectron spectroscopy (XPS), low-energy electron diffraction (LEED), ion-scattering spectroscopy (ISS), and thermal-desorption mass spectroscopy (TDS).[18-19, 37] The methodology followed for the preparation of the $Pt/CeO_2(111)$ surfaces is described in detail in ref. [37] For $Pt/CeO_2(111)$ surfaces, single atoms and small Pt clusters have been observed at low coverages using scanning tunnelling microscopy.[60] In the studies of

methane activation, the sample was transferred *in vacuo* to the reactor at 25 °C, then the reactant gas, 1 Torr of pressure, was introduced. In the experiments of testing the activity of Pt(111) and Pt/CeO_2(111) catalysts for the MDR reaction, the samples were exposed to a mixture of 1 Torr of CH_4 and 1 Torr of CO_2 at room temperature and were rapidly heated to the reaction temperature of 500 °C. Product yields were analysed by mass spectroscopy or gas chromatography. In our experiments, data were collected at intervals of 5 min. The number of molecules (CO and/or H_2) produced in the catalytic tests was normalized by the active area exposed by the sample and the total reaction time. The kinetic experiments were done in the limit of low conversion (< 10%).

AP-XPS measurements were carried out on a commercial SPECS AP-XPS chamber equipped with a PHOIBOS 150 EP MCD-9 analyser at the Chemistry Division of Brookhaven National Laboratory (BNL). In the preparation of the Pt/CeO_2 (111) model catalyst, Ce metal was first evaporated onto a Ru single crystal (0001) at 427 °C in the presence of 5×10^{-7} torr O_2, and then annealed to 527 °C for 10 mins at the same O_2 pressure. The ceria films were estimated to be ca. 4 nm thick (≈10 layers of O-Ce-O) based on the attenuation of the Ru 3d XPS signal. Pt was vapor-deposited on the as-prepared ceria film at 427 °C, and the coverage of Pt was ~ 0.15 ML (monolayer), estimated by the attenuation of the Ce 3d XPS signal. In the studies of MDR on the Pt/CeO_2(111) catalyst, a 50 mTorr CH_4 and 50 mTorr CO_2 gas mixture was used and Ce 3d, Pt 4f spectra were collected at 25, 127, 227, 327, 427 °C. The Ce 3d photoemission line with the strongest Ce^{4+} feature at 916.9 eV was used for the energy calibration of the AP-XPS signals.

Studies with Pt/CeO_2 powder catalysts

Catalyst Preparation. Cerium oxide (CeO_2) was prepared by precipitating white crystalline cerous nitrate ($Ce(NO_3)_3.6H_2O$; Sigma-Aldrich), dissolved in deionised water

with mild stirring. The temperature was kept at 100 °C and ammonia (0.91 $molL^{-1}$) was added drop wise until a pH of 8 was attained. The resulting white slurry precipitate was then collected by filtration, washed with deionised water, and left to dry in an oven at 100 °C for 12 hours. The pale purple dried powder was calcined in a furnace at 500 °C for 4 hours with flowing air. The sample was then ground but not sieved to a consistent powder with a mortar and pestle. The required amount of Pt to make 0.5 wt% Pt/CeO_2 (0.05 g of Pt on 9.95 g of CeO_2) was deposited on CeO_2 by impregnation from a stock solution of 1L/g of Pt cations (from $PtCl_4$ – Sigma-Aldrich) in a beaker at ambient temperature with continuous stirring. The temperature of the beaker was then raised to around 100 °C, while stirring, and retained at this temperature until most of the liquid has vaporized (the complete impregnation process takes about 6-8 hours), to form a paste like material, which was then dried in an oven for 12 hours at 100 °C to remove the remaining water. The dried powder was then calcined in a furnace for 4 hours at 400 °C under flowing air.

Catalytic Performance. In the catalytic performance test of the (0.5 wt%) Pt/CeO_2 powder catalyst for the MDR reaction, a ~12.5 mg sample diluted with a ~30 mg pre-calcined quartz (900 °C) were loaded into a quartz tube and mounted on a flow reactor system. The catalysts were pre-reduced in a 10 cc/min H_2 and 10 cc/min He atmosphere at 400 °C for 40 min before switching to the MDR reaction gas mixture (10 cc/min CH_4, 10 cc/min CO_2 and 10 cc/min N_2, weight hourly space velocity: 180,000 $ml/g_{cat}/h$). The catalysts were then heated stepwise to 700 °C with isothermal steps at 400, 500, 600, and 700 °C for 1 hour. The residual gas products were analysed by a gas chromatography instrument (Agilent 7890A) equipped with flame ionization and thermal conductivity detectors.

XAFS. *In-situ* X-ray absorption near edge structure and (XANES) and extend X-ray absorption fine structure (EXAFS) for the MDR reaction on Pt/CeO_2 were collected at

9BM of the Advanced Photon Source (APS), at Argonne National Laboratory (ANL). Approximately 2 mg catalysts were loaded into a Clausen cell and mounted in line with a gas flow system. The sample was pre-reduced under 5 cc/min H_2 and 5 cc/min He at 400 °C for 40 min, and after cooling down, a 2 cc/min CH_4, 2cc/min CO_2 and 6 cc/min He gas mixture was switched in at room temperature for the MDR reaction. The catalysts were heated stepwise from room temperature to 700 °C with a 10 °C/min ramping rate and Pt L_3-edge spectra were collected e at 300, 500 and 700 °C by a four channel Vortex detector in the fluorescence yield mode. At each temperature stage, tree parallel spectra were collected and averaged together to improve the quality of the data. Data processing was performed using the IFEFFIT package and Pt foil was used as the standard reference for the EXAFS fitting.[61]

AP-XPS. The powder catalyst was pressed onto an aluminium plate and loaded into the AP-XPS chamber. A 10 mTorr of O_2 was introduced and the sample was heated to 400 °C to remove any surface-bounded carbon species before the test. In the studies of MDR on Pt/CeO_2 powder catalyst, the sample was pre-reduced in a 20 mTorr of H_2 at 400 °C for 40 min before switching to a 50 mTorr CH_4 and 50 mTorr CO_2 reaction gas mixture, and Ce 3d and Pt 4f spectra were collected at 25, 127, 227, 327, 427 °C.

XRD. The *in-situ* time-resolved XRD analyses were carried out at 17BM (λ = 0.24108 Å) of the Advanced Photon Source (APS), at Argonne National Laboratory (ANL). A Clausen cell flow reactor was used for the measurement.[62] The reaction conditions were kept the same as the in-situ XAFS measurements and an amorphous Si flat panel (Perkin Elmer) detector was used to collect two-dimensional XRD images throughout the reaction processes. The images were subsequently processed with GSAS-II to obtain diagrams of Intensity versus 2θ. The lattice parameter evolution of ceria was calculated by Rietveld refinement also using GSAS-II.[63] Pt particles or aggregates were not seen in XRD and

TEM for the 0.5 wt% Pt/CeO_2 powder catalyst. The use of low loading is crucial for the comparison of model systems with high surface area catalysts and for defining structure-function relationships.[64]

ASSOCIATE CONTENT

The H_2 TPR results on Pt/CeO_2 powder sample and bare ceria support; AP-XPS signal and the peak fitting at Ce 3d region of 0.15 ML $Pt/CeO_2(111)$ under a pure CH_4 atmosphere at 427 °C; fitting parameters and results of the Ce 3d spectrum; ceria lattice parameter evolution in a CH_4 atmosphere as a function of temperature. This information is available free of charge on the ACS Publications website.

DATA AVAILABILITY

The data that support the plots within these paper and other findings of this study are available from the corresponding authors on reasonable request.

ACKNOWLEDGEMENTS

The research carried out at the Brookhaven National Laboratory (BNL) was supported by the U.S. Department of Energy, Office of Science and Office of Basic Energy Sciences under contract No. DE-SC0012704. The XRD and XAFS experiments carried out at the Advanced Photon Source Beamline 17BM (XRD) and 9BM (XAFS) at Argonne National Laboratory was supported by the U.S. DOE under Contract No. DE-AC02-06CH11357. This project also received funding from the European Union's Horizon 2020 research and innovation programme under the Marie Skłodowska-Curie grant agreement No 832121. M.V.G.P. thanks the support by the MINECO and MICINN-Spain (CTQ2015-71823-R and RTI2018-101604-B-I00, respectively).

References

1. Anderson, T. R.; Hawkins, E.; Jones, P. D., CO_2, the greenhouse effect and global warming: from the pioneering work of Arrhenius and Callendar to today's Earth System Models. *Endeavour* **2016,** *40* (3), 178-187.

2. Schwarz, H.; Shaik, S.; Li, J., Electronic Effects on Room-Temperature, Gas-Phase C–H Bond Activations by Cluster Oxides and Metal Carbides: The Methane Challenge, *J. Am. Chem. Soc*. **2017,** 139 (48),17201-17212.
3. Thornton, P. K., Livestock production: recent trends, future prospects. *Philos. Trans. R. Soc. Lond. B. Biol. Sci.* **2010,** *365* (1554), 2853-2867.
4. Tang, P.; Zhu, Q.; Wu, Z.; Ma, D., Methane activation: the past and future. *Energy Environ. Sci.* **2014,** *7* (8), 2580-2591.
5. Bousquet, P.; Ciais, P.; Miller, J. B.; Dlugokencky, E. J.; Hauglustaine, D. A.; Prigent, C.; Van der Werf, G. R.; Peylin, P.; Brunke, E. G.; Carouge, C.; Langenfelds, R. L.; Lathière, J.; Papa, F.; Ramonet, M.; Schmidt, M.; Steele, L. P.; Tyler, S. C.; White, J., Contribution of anthropogenic and natural sources to atmospheric methane variability. *Nature* **2006,** *443* (7110), 439-443.
6. Arora, S.; Prasad, R., An overview on dry reforming of methane: strategies to reduce carbonaceous deactivation of catalysts. *RSC Adv.* **2016,** *6* (110), 108668-108688.
7. Liu, X,; Sun, L.; Deng, W.-Q., Theoretical Investigation of CO2 Adsorption and Dissociation on Low Index Surfaces of Transition Metals, *J. Phys. Chem. C* **2018**, 122 (11), 8306-8314.
8. Song, Y.; Ozdemir, E.; Ramesh, S.; Adishev, A.; Subramanian, S.; Harale, A.; Albuali, M.; Fadhel, B. A.; Jamal, A.; Moon, D.; Choi, S. H.; Yavuz, C. T., Dry reforming of methane by stable Ni–Mo nanocatalysts on single-crystalline MgO. *Science* **2020,** *367* (6479), 777-781.
9. Vogt, C.; Monai, M.; Sterk, E. B.; Palle, J.; Melcherts, A. E.; Zijlstra, B.; Groeneveld, E.; Berben, P. H.; Boereboom, J. M.; Hensen, E. J., Understanding carbon dioxide activation and carbon–carbon coupling over nickel. *Nat. Commun.* **2019,** *10* (1), 1-10.
10. Weaver, J. F.; Hakanoglu, C.; Antony, A.; Asthagiri, A., Alkane activation on crystalline metal oxide surfaces. *Chem. Soc. Rev.* **2014,** *43* (22), 7536-7547.
11. Tsuji, Y.; Yoshizawa, K., Adsorption and Activation of Methane on the (110) Surface of Rutile-type Metal Dioxides. *J. Phys. Chem. C* **2018,** *122* (27), 15359-15381.
12. Fung, V.; Tao, F.; Jiang, D.-e., Low-temperature activation of methane on doped single atoms: descriptor and prediction. *Phys. Chem. Chem. Phys.* **2018,** *20* (35), 22909-22914.
13. Latimer, A. A.; Kulkarni, A. R.; Aljama, H.; Montoya, J. H.; Yoo, J. S.; Tsai, C.; Abild-Pedersen, F.; Studt, F.; Nørskov, J. K., Understanding trends in C–H bond activation in heterogeneous catalysis. *Nat. Mater.* **2017,** *16* (2), 225-229.
14. Ma, X.; Sun, K.; Liu, J.-X.; Li, W.-X.; Cai, X.; Su, H.-Y., Single Ru Sites-Embedded Rutile TiO2 Catalyst for Non-Oxidative Direct Conversion of Methane: A First-Principles Study. *J. Phys. Chem. C* **2019,** *123* (23), 14391-14397.
15. Pérez-Ramírez, J.; López, N., Strategies to break linear scaling relationships. *Nature Catalysis* **2019,** *2* (11), 971-976.
16. Yuan, K.; Zhong, J.-Q.; Zhou, X.; Xu, L.; Bergman, S. L.; Wu, K.; Xu, G. Q.; Bernasek, S. L.; Li, H. X.; Chen, W., Dynamic oxygen on surface: catalytic intermediate and coking barrier in the modeled CO2 reforming of CH4 on Ni (111). *ACS.Catal.* **2016,** *6* (7), 4330-4339.
17. Rodriguez, J. A.; Zhang, F.; Liu, Z.; Senanayake, S. D., Methane activation and conversion on well-defined metal-oxide Surfaces: in situ studies with synchrotron-based techniques. In *Catalysis: Volume 31*, The Royal Society of Chemistry: 2019; Vol. 31, pp 198-215.

18. Lustemberg, P. G.; Ramírez, P. J.; Liu, Z.; Gutiérrez, R. A.; Grinter, D. G.; Carrasco, J.; Senanayake, S. D.; Rodriguez, J. A.; Ganduglia-Pirovano, M. V., Room-Temperature Activation of Methane and Dry Re-forming with CO2 on Ni-CeO2(111) Surfaces: Effect of Ce3+ Sites and Metal–Support Interactions on C–H Bond Cleavage. *ACS.Catal.* **2016,** *6* (12), 8184-8191.
19. Liu, Z.; Lustemberg, P.; Gutiérrez, R. A.; Carey, J. J.; Palomino, R. M.; Vorokhta, M.; Grinter, D. C.; Ramírez, P. J.; Matolín, V.; Nolan, M.; Ganduglia-Pirovano, M. V.; Senanayake, S. D.; Rodriguez, J. A., In Situ Investigation of Methane Dry Reforming on Metal/Ceria(111) Surfaces: Metal–Support Interactions and C−H Bond Activation at Low Temperature. *Angew. Chem. Int. Ed.* **2017,** *56* (42), 13041-13046.
20. Lustemberg, P. G.; Palomino, R. M.; Gutierrez, R. A.; Grinter, D. C.; Vorokhta, M.; Liu, Z. Y.; Ramirez, P. J.; Matolin, V.; Ganduglia-Pirovano, M. V.; Senanayake, S. D.; Rodriguez, J. A., Direct Conversion of Methane to Methanol on Ni-Ceria Surfaces: Metal-Support Interactions and Water-Enabled Catalytic Conversion by Site Blocking. *J. Am. Chem. Soc.* **2018,** *140* (24), 7681-7687.
21. Besenbacher, F.; Chorkendorff, I.; Clausen, B.; Hammer, B.; Molenbroek, A.; Nørskov, J. K.; Stensgaard, I., Design of a surface alloy catalyst for steam reforming. *Science* **1998,** *279* (5358), 1913-1915.
22. Rostrupnielsen, J.; Hansen, J. B., CO2-reforming of methane over transition metals. *J. Catal.* **1993,** *144* (1), 38-49.
23. Womes, M.; Cholley, T.; Le Peltier, F.; Morin, S.; Didillon, B.; Szydlowski-Schildknecht, N., Study of the reaction mechanisms between Pt (acac) 2 and alumina surface sites: Application to a new refilling technique for the controlled variation of the particle size of Pt/Al2O3 catalysts. *Appl. Catal., A* **2005,** *283* (1-2), 9-22.
24. Ballarini, A.; Basile, F.; Benito, P.; Bersani, I.; Fornasari, G.; De Miguel, S.; Maina, S.; Vilella, J.; Vaccari, A.; Scelza, O., Platinum supported on alkaline and alkaline earth metal-doped alumina as catalysts for dry reforming and partial oxidation of methane. *Appl. Catal., A* **2012,** *433*, 1-11.
25. Elsayed, N. H.; Roberts, N. R.; Joseph, B.; Kuhn, J. N., Low temperature dry reforming of methane over Pt–Ni–Mg/ceria–zirconia catalysts. *Appl. Catal., B* **2015,** *179*, 213-219.
26. Zhu, Y.; Chen, K.; Yi, C.; Mitra, S.; Barat, R., Dry reforming of methane over palladium–platinum on carbon nanotube catalyst. *Chem. Eng. Commun.* **2018,** *205* (7), 888-896.
27. Damyanova, S.; Pawelec, B.; Arishtirova, K.; Huerta, M. M.; Fierro, J., The effect of CeO2 on the surface and catalytic properties of Pt/CeO2–ZrO2 catalysts for methane dry reforming. *Appl. Catal., B* **2009,** *89* (1-2), 149-159.
28. Wu, H.; Pantaleo, G.; La Parola, V.; Venezia, A. M.; Collard, X.; Aprile, C.; Liotta, L. F., Bi-and trimetallic Ni catalysts over Al2O3 and Al2O3-MOx (M= Ce or Mg) oxides for methane dry reforming: Au and Pt additive effects. *Appl. Catal., B* **2014,** *156*, 350-361.
29. García-Diéguez, M.; Pieta, I.; Herrera, M.; Larrubia, M.; Alemany, L., Nanostructured Pt-and Ni-based catalysts for CO2-reforming of methane. *J. Catal.* **2010,** *270* (1), 136-145.
30. Choudhary, T. V.; Aksoylu, E.; Wayne Goodman, D., Nonoxidative activation of methane. *Cat. Rev. - Sci. Eng.* **2003,** *45* (1), 151-203.
31. Schoofs, G. R.; Arumainayagam, C. R.; McMaster, M. C.; Madix, R. J., Dissociative chemisorption of methane on Pt(111). *Surf. Sci.* **1989,** *215* (1), 1-28.

32. Marsh, A. L.; Becraft, K. A.; Somorjai, G. A., Methane dissociative adsorption on the Pt (111) surface over the 300− 500 K temperature and 1− 10 Torr pressure ranges. *J. Phys. Chem. B* **2005,** *109* (28), 13619-13622.
33. Petersen, M. A.; Jenkins, S. J.; King, D. A., Theory of Methane Dehydrogenation on Pt {110}(1× 2). Part I: Chemisorption of CH x (x= 0− 3). *J. Phys. Chem. B* **2004,** *108* (19), 5909-5919.
34. Nave, S.; Tiwari, A. K.; Jackson, B., Methane dissociation and adsorption on Ni (111), Pt (111), Ni (100), Pt (100), and Pt (110)-(1× 2): energetic study. *J. Chem. Phys.* **2010,** *132* (5), 054705.
35. Daelman, N.; Capdevila-Cortada, M.; López, N., Dynamic charge and oxidation state of Pt/CeO2 single-atom catalysts. *Nat. Mater.* **2019,** *18* (11), 1215-1221.
36. Brummel, O.; Waidhas, F.; Faisal, F.; Fiala, R.; Vorokhta, M.; Khalakhan, I.; Dubau, M.; Figueroba, A.; Kovács, G.; Aleksandrov, H. A.; Vayssilov, G. N.; Kozlov, S. M.; Neyman, K. M.; Matolín, V.; Libuda, J., Stabilization of Small Platinum Nanoparticles on Pt–CeO2 Thin Film Electrocatalysts During Methanol Oxidation. *J. Phys. Chem. C* **2016,** *120* (35), 19723-19736.
37. Bruix, A.; Rodriguez, J. A.; Ramírez, P. J.; Senanayake, S. D.; Evans, J.; Park, J. B.; Stacchiola, D.; Liu, P.; Hrbek, J.; Illas, F., A New Type of Strong Metal–Support Interaction and the Production of H2 through the Transformation of Water on Pt/CeO2(111) and Pt/CeOx/TiO2(110) Catalysts. *J. Am. Chem. Soc.* **2012,** *134* (21), 8968-8974.
38. Paffett, M.; Gebhard, S.; Windham, R.; Koel, B., Chemisorption of carbon monoxide, hydrogen, and oxygen on ordered tin/platinum (111) surface alloys. *J. Phys. Chem.* **1990,** *94* (17), 6831-6839.
39. Pirug, G.; Bonzel, H.; Brodén, G., The adsorption of potassium on Pt (111) and its effect on oxygen adsorption. *Surf. Sci.* **1982,** *122* (1), 1-20.
40. Pereira-Hernández, X. I.; DeLaRiva, A.; Muravev, V.; Kunwar, D.; Xiong, H.; Sudduth, B.; Engelhard, M.; Kovarik, L.; Hensen, E. J. M.; Wang, Y.; Datye, A. K., Tuning Pt-CeO2 interactions by high-temperature vapor-phase synthesis for improved reducibility of lattice oxygen. *Nat. Commun.* **2019,** *10* (1), 1358.
41. Dvořák, F.; Farnesi Camellone, M.; Tovt, A.; Tran, N.-D.; Negreiros, F. R.; Vorokhta, M.; Skála, T.; Matolínová, I.; Mysliveček, J.; Matolín, V.; Fabris, S., Creating single-atom Pt-ceria catalysts by surface step decoration. *Nat. Commun.* **2016,** *7* (1), 10801.
42. Lustemberg, P. G.; Zhang, F.; Gutiérrez, R. A.; Ramírez, P. J.; Senanayake, S. D.; Rodriguez, J. A.; Ganduglia-Pirovano, M. V., Breaking Simple Scaling Relations through Metal–Oxide Interactions: Understanding Room-Temperature Activation of Methane on M/CeO2 (M = Pt, Ni, or Co) Interfaces. *J. Phys. Chem. Lett.* **2020,** *11* (21), 9131-9137.
43. Dablemont, C.; Lang, P.; Mangeney, C.; Piquemal, J.-Y.; Petkov, V.; Herbst, F.; Viau, G., FTIR and XPS Study of Pt Nanoparticle Functionalization and Interaction with Alumina. *Langmuir* **2008,** *24* (11), 5832-5841.
44. Fu, X.; Wang, Y.; Wu, N.; Gui, L.; Tang, Y., Surface Modification of Small Platinum Nanoclusters with Alkylamine and Alkylthiol: An XPS Study on the Influence of Organic Ligands on the Pt 4f Binding Energies of Small Platinum Nanoclusters. *J. Colloid Interface Sci.* **2001,** *243* (2), 326-330.
45. Mullins, D. R., The surface chemistry of cerium oxide. *Surf. Sci. Rep.* **2015,** *70* (1), 42-85.

46. Nishiyama, N.; Yamazaki, S., Effect of mixed valence states of platinum ion dopants on the photocatalytic activity of titanium dioxide under visible light irradiation. *ACS omega* **2017,** *2* (12), 9033-9039.
47. Guda, A. A.; Bugaev, A. L.; Kopelent, R.; Braglia, L.; Soldatov, A. V.; Nachtegaal, M.; Safonova, O. V.; Smolentsev, G., Fluorescence-detected XAS with sub-second time resolution reveals new details about the redox activity of Pt/CeO2 catalyst. *J. Synchrotron Radiat.* **2018,** *25* (4), 989-997.
48. Setthapun, W.; Williams, W. D.; Kim, S. M.; Feng, H.; Elam, J. W.; Rabuffetti, F. A.; Poeppelmeier, K. R.; Stair, P. C.; Stach, E. A.; Ribeiro, F. H., Genesis and evolution of surface species during Pt atomic layer deposition on oxide supports characterized by in situ XAFS analysis and water− gas shift reaction. *J. Phys. Chem. C* **2010,** *114* (21), 9758-9771.
49. Uemura, Y.; Inada, Y.; Bando, K. K.; Sasaki, T.; Kamiuchi, N.; Eguchi, K.; Yagishita, A.; Nomura, M.; Tada, M.; Iwasawa, Y., In situ time-resolved XAFS study on the structural transformation and phase separation of Pt3Sn and PtSn alloy nanoparticles on carbon in the oxidation process. *Phys. Chem. Chem. Phys.* **2011,** *13* (35), 15833-15844.
50. Akri, M.; Zhao, S.; Li, X.; Zang, K.; Lee, A. F.; Isaacs, M. A.; Xi, W.; Gangarajula, Y.; Luo, J.; Ren, Y., Atomically dispersed nickel as coke-resistant active sites for methane dry reforming. *Nat. Commun.* **2019,** *10* (1), 1-10.
51. Tang, Y.; Wei, Y.; Wang, Z.; Zhang, S.; Li, Y.; Nguyen, L.; Li, Y.; Zhou, Y.; Shen, W.; Tao, F. F.; Hu, P., Synergy of Single-Atom Ni1 and Ru1 Sites on CeO2 for Dry Reforming of CH4. *J. Am. Chem. Soc.* **2019,** *141* (18), 7283-7293.
52. Turap, Y.; Wang, I.; Fu, T.; Wu, Y.; Wang, Y.; Wang, W., Co–Ni alloy supported on CeO2 as a bimetallic catalyst for dry reforming of methane. *Int. J. Hydrogen Energ.* **2020,** *45* (11), 6538-6548.
53. Rameshan, C.; Li, H.; Anic, K.; Roiaz, M.; Pramhaas, V.; Rameshan, R.; Blume, R.; Hävecker, M.; Knudsen, J.; Knop-Gericke, A., In situ NAP-XPS spectroscopy during methane dry reforming on ZrO2/Pt (1 1 1) inverse model catalyst. *J. Phys.: Condens. Matter* **2018,** *30* (26), 264007.
54. Zhang, F.; Liu, Z.; Chen, X.; Rui, N.; Betancourt, L. E.; Lin, L.; Xu, W.; Sun, C.-j.; Abeykoon, A. M. M.; Rodriguez, J. A.; Teržan, J.; Lorber, K.; Djinović, P.; Senanayake, S. D., Effects of Zr Doping into Ceria for the Dry Reforming of Methane over Ni/CeZrO2 Catalysts: In Situ Studies with XRD, XAFS, and AP-XPS. *ACS.Catal.* **2020,** *10* (5), 3274-3284.
55. Wolfbeisser, A.; Sophiphun, O.; Bernardi, J.; Wittayakun, J.; Föttinger, K.; Rupprechter, G., Methane dry reforming over ceria-zirconia supported Ni catalysts. *Catal. Today* **2016,** *277*, 234-245.
56. Weaver, J. F.; Carlsson, A. F.; Madix, R. J., The adsorption and reaction of low molecular weight alkanes on metallic single crystal surfaces. *Surf. Sci. Rep.* **2003,** *50* (4-5), 107-199.
57. Freund, H.-J.; Roberts, M. W., Surface chemistry of carbon dioxide. *Surf. Sci. Rep.* **1996,** *25* (8), 225-273.
58. Dai, C.; Zhang, S.; Zhang, A.; Song, C.; Shi, C.; Guo, X., Hollow zeolite encapsulated Ni–Pt bimetals for sintering and coking resistant dry reforming of methane. *J. Mater. Chem. A* **2015,** *3* (32), 16461-16468.
59. Chen, L.; Huang, Q.; Wang, Y.; Xiao, H.; Liu, W.; Zhang, D.; Yang, T., Tailoring performance of Co–Pt/MgO–Al2O3 bimetallic aerogel catalyst for methane oxidative

carbon dioxide reforming: Effect of Pt/Co ratio. *Int. J. Hydrogen Energy* **2019,** *44* (36), 19878-19889.
60. Parkinson, G. S., Unravelling single atom catalysis: The surface science approach. *Chinese J. Catal.* **2017,** *38* (9), 1454-1459.
61. Ravel, B.; Newville, M., ATHENA, ARTEMIS, HEPHAESTUS: data analysis for X-ray absorption spectroscopy using IFEFFIT. *J. Synchrotron Radiat.* **2005,** *12* (4), 537-541.
62. Chupas, P. J.; Chapman, K. W.; Kurtz, C.; Hanson, J. C.; Lee, P. L.; Grey, C. P., A versatile sample-environment cell for non-ambient X-ray scattering experiments. *J. Appl. Crystallogr.* **2008,** *41* (4), 822-824.
63. Toby, B. H.; Von Dreele, R. B., GSAS-II: the genesis of a modern open-source all purpose crystallography software package. *J. Appl. Crystallogr.* **2013,** *46* (2), 544-549.
64. Resasco, J.; DeRita, L.; Dai, S.; Chada, J. P.; Xu, M.; Yan, X.; Finzel, J.; Hanukovich, S.; Hoffman, A. S.; Graham, G. W.; Bare, S. R.; Pan, X.; Christopher, P., Uniformity Is Key in Defining Structure–Function Relationships for Atomically Dispersed Metal Catalysts: The Case of Pt/CeO2. *J. Am. Chem. Soc.* **2020,** *142* (1), 169-184.

Figure captions

Figure 1. He-II valence UPS spectra collected before and after deposition of 0.15 ML of Pt on a $CeO_2(111)$ surface.

Figure 2. Top panel: C 1s XPS spectra collected after exposing plain $CeO_2(111)$ and $Pt/CeO_2(111)$ surfaces to 1 Torr of methane at 25 °C for 5 minutes. Bottom panel: Variation in the signal for CH_x and CO_x species in the C 1s region as a function of admetal coverage in $Pt/CeO_2(111)$.

Figure 3. C 1s XPS spectra collected after exposing plain $CeO_2(111)$ and a $Pt/CeO_2(111)$ surface to 1 Torr of CO_2 at 25 °C for 5 minutes. The carbonate (CO_x) peak did not disappear when the surfaces were heated to temperatures as high as 500 °C.

Figure 4. Production of H_2 by methane dry reforming on Pt(111) and 0.15 ML of Pt supported on $CeO_2(111)$. Reaction conditions: 1 Torr of CH_4, 1 Torr of CO_2 and 500 °C.

Figure 5. Calculated turnover frequencies for $Pt/CeO_2(111)$ surfaces. For comparison, the initial TOF of Pt(111), before it was deactivated by carbon deposition, is included as the dashed line at the bottom. Reaction conditions: 1 Torr of CH_4, 1 Torr of CO_2 and 500 °C.

Figure 6. Ce 3d and Pt 4f AP-XPS spectra of Pt/CeO_2 (111) for the MDR reaction at elevated temperatures. Reaction condition: a 100 mTorr CH_4 + CO_2 1:1 gas mixture was introduced into reaction chamber after Pt deposition, and the spectra were collected at 25, 127, 227, 327 and 427 °C under this gas mixture

Figure 7. Catalytic performance of 0.5 wt% Pt/CeO_2 catalyst for the MDR reaction at different temperatures (400-700 ºC). The catalyst was pre-reduced in H_2 to generate active metallic Pt, and the flow reactor condition for MDR:10 cc/min CO_2 + 10 cc/min CH_4 + 30 cc/min N_2 gas mixture; weight hourly space velocity (WHSV): 180, 000 ml/(g_{cat}·h).

Figure 8. Ce 3d and Pt 4f AP-XPS spectra of 0.5 wt% Pt/CeO_2 for the MDR reaction at elevated temperatures. A 10 mTorr O_2 and a 20 mTorr of H_2 were used to pretreat the sample at 400 °C sequentially to remove the surface-bounded carbon species and reduce the sample, respectively.

Figure 9. Pt L_3 in-situ XANES (a) and the Fourier transformed EXAFS region (b) of the sample during the MDR reaction at different temperatures. For comparison, we also include data for a Pt foil and a PtO_2 powder.

Figure 10. (a). Time resolved *in-situ* XRD profile of Pt/CeO_2 and (b) ceria lattice parameter evolution under the MDR reaction. Reaction condition: around 2 mg catalyst was pretreated in H_2 at 400 °C for 40 min before switching the gas to a mixture of 2 cc/min CO_2 + 2 cc/min CH_4 + 6 cc/min He at room temperature. The sample was then heated under MDR reaction atmosphere from 25 to 700 °C with a 10 °C/min ramping rate and 30 min soak time at each temperature stage of 300, 400, 500, 600, and 700 °C.

Figure 11. Catalytic activity for MDR on Cu-, Ni-, Co- and Pt/CeO_2 catalysts (~0.15 ML of admetal). Amounts of H_2 formed after exposing the catalysts to 1 Torr of CH_4 and 1 Torr of CO_2 at 650 K for 5 minutes.